1 **Degradation Kinetics and Secondary Organic Aerosol Formation**

2 **from Eugenol by Hydroxyl Radicals**

3 Changgeng Liu[1,2], Yongchun Liu[1,3,4,a,*], Tianzeng Chen[1,4], Jun Liu[1,4], Hong He[1,3,4,*]

4 [1]State Key Joint Laboratory of Environment Simulation and Pollution Control,

5 Research Center for Eco-Environmental Sciences, Chinese Academy of Sciences,

6 Beijing 100085, China

7 [2]School of Biological and Chemical Engineering, Panzhihua University, Panzhihua

8 617000, China

9 [3]Center for Excellence in Regional Atmospheric Environment, Institute of Urban

10 Environment, Chinese Academy of Sciences, Xiamen 361021, China

11 [4]University of Chinese Academy of Sciences, Beijing 100049, China

12 [a]Currently at: Beijing Advanced Innovation Center for Soft Matter Science and

13 Engineering, Beijing University of Chemical Technology, Beijing 100029, China

14 *Correspondence to*: Yongchun Liu (liuyc@buct.edu.cn) and Hong He

15 (honghe@rcees.ac.cn)

Atmospheric
Chemistry
and Physics
Discussions

16   **Abstract.** Methoxyphenols are an important organic component of wood-burning

17   emissions and considered to be potential precursors of secondary organic aerosols

18   (SOA). In this work, the rate constant and SOA formation potential for the OH-initiated

19   reaction of 4-allyl-2-methoxyphenol (eugenol) were investigated for the first time in an

20   oxidation flow reactor (OFR). The rate constant was $(8.01 \pm 0.40) \times 10^{-11}$ cm^3 molecule^{-1} s^{-1} as determined by the relative rate method. The SOA yield first increased and then

22   decreased as a function of OH exposure, and was also dependent on eugenol

23   concentration. The maximum SOA yields (0.11−0.31) obtained at different eugenol

24   concentrations could be expressed well by an one-product model. The carbon oxidation

25   state (OS_C) increased linearly and significantly as OH exposure rose, indicating that a

26   high oxidation degree was achieved for SOA. In addition, the presence of SO_2 (0−198

27   ppbv) and NO_2 (0−109 ppbv) was conducive to increasing SOA yield, for which the

28   maximum enhancement values were 38.57% and 19.17%, respectively. The N/C ratio

29   (0.032−0.043) indicated that NO_2 participated in the OH-initiated reaction,

30   subsequently forming organic nitrates. The results could be helpful for further

31   understanding the SOA formation potential from the atmospheric oxidation of

32   methoxyphenols and the atmospheric aging process of smoke plumes from biomass-

33   burning emissions.

Atmospheric
Chemistry
and Physics
Discussions

Open Access

1 Introduction

34

35 Wood combustion is a major contributor to atmospheric fine particulate matter (PM)

36 (Bruns et al., 2016), which could contribute approximately 10−50% of the total organic

37 fraction of atmospheric aerosols (Schauer and Cass, 2000). In some regions with cold

38 climates, wood smoke-associated aerosols are estimated to account for more than 70%

39 of $PM_{2.5}$ in winter (Jeong et al., 2008; Ward et al., 2006). Recently, significant potential

40 of secondary organic aerosol (SOA) formation from wood smoke emissions has been

41 reported (Bruns et al., 2016; Gilardoni et al., 2016; Tiitta et al., 2016; Ciarelli et al.,

42 2017; Ding et al., 2017). In addition, the organic compounds derived from wood

43 combustion and their oxidation products may contribute significantly to global

44 warming due to their light-absorbing properties (Chen and Bond, 2010). It has been

45 reported that wood smoke particles are predominant in the inhalable size range (Bari et

46 al., 2010) and that their extracts are mutagenic (Kleindienst et al., 1986). Exposure to

47 wood smoke can result in adverse health effects associated with acute respiratory

48 infections, tuberculosis, lung cancer, cataracts, etc. (Bolling et al., 2009). Therefore,

49 wood combustion has multifaceted impacts on climate, air quality, and human health.

50   Methoxyphenols produced by lignin pyrolysis are potential tracers for wood smoke,

51 and their emission rates are in the range of 900−4200 mg kg^{-1} fuel (Schauer et al., 2001;

52 Simpson et al., 2005; Nolte et al., 2001). The highest level of methoxyphenols in the

53 atmosphere always appears during a wood smoke-dominated period, with observed

54 values up to several mg m^{-3} (Schauer and Cass, 2000; Schauer et al., 2001; Simpson et

55 al., 2005). Methoxyphenols are semi-volatile aromatic compounds with low molecular

56 weight, and many of them are found to mainly exist in the gas phase at typical ambient

57 temperature (Simpson et al., 2005; Schauer et al., 2001). Thus, methoxyphenols can be

58 chemically transformed through gas-phase reactions with atmospheric oxidants (Coeur-

59 Tourneur et al., 2010a; Lauraguais et al., 2012, 2014a, 2014b, 2015, 2016; Yang et al.,

60 2016; Zhang et al., 2016; El Zein et al., 2015). The corresponding rate constants control

61 their effectiveness as stable tracers for wood combustion and atmospheric lifetimes. In

62 recent years, the rate constants for the gas-phase reactions of some methoxyphenols

63 with hydroxyl (OH) radicals (Coeur-Tourneur et al., 2010a; Lauraguais et al., 2012,

64 2014b, 2015), nitrate (NO_3) radicals (Lauraguais et al., 2016; Yang et al., 2016; Zhang

65 et al., 2016), chlorine atoms (Cl) (Lauraguais et al., 2014a) and ozone (O_3) (El Zein et

66 al., 2015) have been determined. Some studies have indicated significant SOA

67 formation from 2,6-dimethoxyphenol (syringol) and 2-methoxyphenol (guaiacol) with

68 respect to their reactions with OH radicals (Sun et al., 2010; Lauraguais et al., 2012,

69 2014b; Ahmad et al., 2017; Yee et al., 2013; Ofner et al., 2011). Although biomass-

70 burning emissions have been indicated to have great SOA formation potential via

71 atmospheric oxidation (Bruns et al., 2016; Gilardoni et al., 2016; Li et al., 2017; Ciarelli

72 et al., 2017; Ding et al., 2017), SOA formation and growth from methoxyphenols are

73 still poorly understood. Besides, the observed SOA levels in the atmosphere cannot be

74 well explained by the present knowledge on SOA formation, which reflects the fact that

75 a large number of precursors are not taken into account in the SOA-formation reactions

Atmospheric
Chemistry
and Physics
Discussions

76   included in the atmospheric models (Lauraguais et al., 2012).

77   4-Allyl-2-methoxyphenol (eugenol), a type of methoxyphenols, is a typical

78   compound produced by ligin pyrolysis with a branched alkene group, and is widely

79   detected in the atmosphere (Schauer et al., 2001; Simpson et al., 2005; Bari et al., 2009).

80   Its average emission concentration and factor in beech burning are 0.032 $\mu g\ m^{-3}$ and

81   1.52 $\mu g\ g^{-1}$ PM, respectively, which are both higher than those (0.016 $\mu g\ m^{-3}$ and 0.762

82    $\mu g\ g^{-1}$ PM) of guaiacol (Bari et al., 2009). It has even be detected in human urine after

83   exposure to wood smoke (Dills et al., 2006). Eugenol has been observed to mainly

84   distribute in the gas phase in wood smoke emissions (Schauer et al., 2001), and its

85   gas/particle-partition coefficient is lower than 0.01 (Zhang et al., 2016), thus indicating

86   the importance of its gas-phase reactions in the atmosphere. For this reason, the aim of

87   this work was to determine the rate constant and explore the SOA formation potential

88   for eugenol in the gas-phase reaction with OH radicals using an Oxidation Flow Reactor

89   (OFR). In addition, the effects of SO_2 and NO_2 on SOA formation were investigated.

90   To our knowledge, this work represents the first determination of the rate constant and

91   SOA yield for the gas-phase reaction of eugenol with OH radicals.

92   **2   Experimental section**

93   The detailed schematic description of the experimental system used in this work is

94   shown in Figs. S1 and S2. The gas-phase reactions were conducted in the OFR, whose

95   detailed description has been presented elsewhere (Liu et al., 2014). Before entering

96   into the OFR, gas-phase species were mixed thoroughly in the mixing tube. The

Atmospheric
Chemistry
and Physics
Discussions

97   reaction time in the OFR was 26.7 s, calculated according to the illuminated volume

98   (0.89 L) and the total flow rate (2 L min^{-1}). OH radicals were generated by photolysis

99   of O_3 in the presence of water vapor using a 254 nm UV lamp (Jelight Co., Inc.), and

100   their formation reactions have been described elsewhere (Zhang et al., 2017). The

101   concentration of OH radicals was governed by O_3 concentration and relative humidity

102   (RH). O_3 concentration was controlled by changing the unshaded length of a 185 nm

103   UV lamp (Jelight Co., Inc.). O_3 was produced by passing zero air through an O_3

104   generator (Model 610-220, Jelight Co., Inc.), and its concentration was in the range of

105   0.94−9.11 ppmv in this work measured with an O_3 analyzer (Model 205, 2B Technology

106   Inc.). RH and temperature in the OFR were (44.0 ±2.0)% and (301 ±1) K, respectively,

107   measured at the outlet of the OFR. The steady-state concentrations of OH radicals were

108   determined using SO_2 as the reference compound in separate calibration experiments.

109   It is a widely-used method for calculating OH exposure in the OFR, but could not well

110   describe the potential OH suppression caused by the added external OH reactivity

111   (Zhang et al., 2017; Lambe et al., 2015; Simonen et al., 2017; Li et al., 2015; Peng et

112   al., 2015, 2016). The decay of SO_2 from its reaction with OH radicals (9×10^{-13} cm^3

113   molecule^{-1} s^{-1}) (Davis et al., 1979) was measured by a SO_2 analyzer (Model 43i, Thermo

114   Fisher Scientific Inc.). The concentration of OH radicals ([OH]) in this work ranged

115   from approximate 4.5×10^9 to 4.7×10^{10} molecules cm^{-3}, and the corresponding OH

116   exposures were in the range of 1.21−12.55 $\times 10^{11}$ molecules cm^{-3} s or approximate 0.93

117   to 9.68 d of equivalent atmospheric exposure.

Atmospheric
Chemistry
and Physics
Discussions

118   An Aerodyne high-resolution time-of-flight aerosol mass spectrometer (HR-ToF-

119   AMS) was applied to perform online measurement of the chemical composition of

120   particles and the non-refractory submicron aerosol mass (DeCarlo et al., 2006). The

121   size distribution and concentration of particles were monitored by a scanning mobility

122   particle sizer (SMPS), consisting of a differential mobility analyzer (DMA) (Model

123   3082, TSI Inc.) and a condensation particle counter (CPC) (Model 3776, TSI Inc.).

124   Assuming that particles are spherical and non-porous, the average effective particle

125   density could be calculated to be 1.5 g cm^{-3} using the equation $\rho=d_{va}/d_m$ (DeCarlo et al.,

126   2004), where d_{va} is the mean vaccum aerodynamic diameter measured by HR-ToF-

127   AMS and d_m is the mean volume-weighted mobility diameter measured by SMPS. The

128   mass concentration of particles measured by HR-ToF-AMS was corrected by SMPS

129   data in this work using the same method as Gordon et al. (2014). Eugenol and reference

130   compounds were measured by a proton-transfer reaction time-of-flight mass

131   spectrometer (PTR-QiToF-MS) (Ionicon Analytik GmbH). More experimental details

132   were described in the supplementary information.

133   **3   Results and discussion**

134   **3.1   Rate constant**

135   In order to investigate the possible photolysis of eugenol and reference compounds at

136   254 nm UV light in the OFR, the comparative experiments were conducted with UV

137   lamp turned on and turned off. The normalized mass spectra of eugenol and reference

138   compounds in the dark and light were shown in Fig. S3. The results showed that no

Atmospheric
Chemistry
and Physics
Discussions

Open Access

139   significant decay (<5%) by photolysis was observed and could be neglected. According

140   to the results reported by Peng et al. (2016), the photolysis of phenol and 1,3,5-

141   trimethylbenzene could be ignored when the ratio of exposure to 254 nm and OH is

142   lower than 1×10^6 cm s^{-1}, of which value in this work also met this condition. In addition,

143   the initial concentration of eugenol was determined with UV lamp turned on. Therefore,

144   the effect of photolysis could be neglected in this work.

145   The rate constant for the gas-phase reaction of eugenol with OH radicals was

146   determined by the relative rate method, which can be expressed as the following

147   equation (Coeur-Tourneur et al., 2010a; Yang et al., 2016; Zhang et al., 2016):

148    $\ln(C_{E0}/C_{Et}) = \ln(C_{R0}/C_{Rt})k_E / k_R$ (1)

149   where C_{E0} and C_{Et} are the initial and real-time concentrations of eugenol, respectively.

150   k_E is the rate constant of the eugenol reaction with OH radicals. C_{R0} and C_{Rt} are the

151   initial and real-time concentrations of reference compound, respectively. k_R is the rate

152   constant of the reference compound with OH radicals, of which values for m-xylene

153   and 1,3,5-trimethylbenzene are 2.20×10^{-11} and 5.67×10^{-11} cm^3 molecule^{-1} s^{-1},

154   respectively (Kramp and Paulson, 1998; Coeur-Tourneur et al., 2010a).

155   Data obtained from the reactions were plotted in the form of Eq. (1) and were well

156   fitted by linear regression ($R^2 > 0.97$, Fig. 1). A summary of the slopes and the rate

157   constants are listed in Table 1. The errors in k_E/k_R are the standard deviations generated

158   from the linear regression analysis and do not include the uncertainty in the rate

159   constants of the reference compounds. The rate constants are $(7.54 \pm 0.28) \times 10^{-11}$ and

Atmospheric
Chemistry
and Physics
Discussions

160    $(8.47 \pm 0.51) \times 10^{-11}$ cm^3 molecule^{-1} s^{-1}, respectively, when using 1,3,5-

161   trimethylbenzene and m-xylene as reference compounds. According to the US EPA

162   AOP WIN model based on the structure activity relationship (SAR) (US EPA, 2012)

163   the rate constant was calculated to be 6.50×10^{-11} cm^3 molecule^{-1} s^{-1} (Table 1), which

164   is lower than that obtained in this work. Inaccurate performance of the AOP WIN model

165   has been observed for other multifunctional organics due to the inaccurate

166   representation of the eletronic effects of different functional groups on reactivity

167   (Coeur-Tourneur et al., 2010a; Lauraguais et al., 2012). This suggests that it is necessary

168   to determine the rate constants of multifunctional organics through lab experiments.

169   The rate constant determined in this work can be used to calculate the atmospheric

170   lifetime of eugenol with respect to its reaction with OH radicals. Assuming a typical

171   [OH] for a 24 h average value to be 1.5×10^6 molecules cm^{-3} (Mao et al., 2009), the

172   corresponding lifetime of eugenol was calculated to be 2.31 h with the average rate

173   constant of 8.01×10^{-11} cm^3 molecule^{-1} s^{-1}. This short lifetime indicates that eugenol is

174   too reactive to be used as a tracer for wood smoke emissions, and also implies the

175   possible fast conversion of eugenol from gas-phase to secondary aerosol during the

176   transportation process.

177   The rate constant obtained in this work is about 2 orders of magnitude faster than

178   that for eugenol with NO$_3$ radicals (1.6×10^{-13} cm^3 molecule^{-1} s^{-1}) (Zhang et al., 2016),

179   which suggests that the OH-initiated reaction of eugenol might be the main chemical

180   transformation in the atmosphere. The rate constants of the OH-initiated reactions of

Atmospheric
Chemistry
and Physics
Discussions

181   guaiacol, 2,6-dimethylphenol, and syringol were 7.53×10^{-11}, 6.70×10^{-11}, and $9.66 \times$

182   10^{-11} cm^3 molecule^{-1} s^{-1}, respectively (Coeur-Tourneur et al., 2010a; Thuner et al., 2004;

183   Lauraguais et al., 2012). The reactivity of eugenol toward OH radicals is slightly higher

184   than those of guaiacol and 2,6-dimethylphenol, while slightly slower than that of

185   syringol. The presence of two methoxyl groups ($-OCH_3$) in syringol activates the

186   electrophilic addition of OH radicals to the benzene ring by donating electron density

187   through the resonance effect (Lauraguais et al., 2016). The activation effect of the

188   methoxyl group is much larger than those of alkyl groups (McMurry, 2004). In a recent

189   study, the reported energy barrier of NO_3 electrophilic addition to eugenol was about 2-

190   fold than that of 4-ethylguaiacol, indicating that the activation effect of the allyl group

191   ($-CH_2CH=CH_2$) is lower than that of the ethyl group ($-CH_2CH_3$) (Zhang et al., 2016).

192   These results are in accordance with the activation effects of the substituants toward the

193   electrophilic addition of OH radicals (McMurry, 2004).

194   **3.2 Effects of eugenol concentration and OH exposure on SOA formation**

195   In this work, a series of experiments were conducted in the OFR with different eugenol

196   concentrations. The SOA yield was determined as the ratio of the SOA mass

197   concentration (M_0, µg m^{-3}) to the reacted eugenol concentration (Δ[eugenol], µg m^{-3})

198   (Kang et al., 2007). The experimental conditions and maximum SOA yields are listed

199   in Table 2. Fig. S4 shows the plots of the SOA yield versus OH exposure at different

200   eugenol concentrations. Higher concentrations resulted in higher amounts of

201   condensable products and subsequently increased SOA yield (Lauraguais et al., 2012).

Atmospheric
Chemistry
and Physics
Discussions

Open Access

202   SOA mass also directly influences the gas/particle partitioning, because SOA can serve

203   as the adsorption medium for oxidation products, and higher SOA mass generally

204   results in higher SOA yield (Lauraguais et al., 2012, 2014b). In the OFR, in all cases

205   the SOA yield first increased and then decreased as a function of OH exposure (Fig.

206   S4). This trend is the most common phenomenon observed in PAM reactor studies

207   (Lambe et al., 2015; Ortega et al., 2016; Simonen et al., 2017). In this work, according

208   to the SO_2 decay in the presence of eugenol and the OFR exposure estimator (v2.3)

209   developed by Jimenez's group based on the estimation equations reported in the

210   previous work (Li et al., 2015; Peng et al., 2015, 2016), the maximum reduction of OH

211   exposure by eugenol in the OFR was approximately 30%. Although OH suppression by

212   eugenol was not well determined in the OFR for the positive influence of SO_2 on SOA

213   formation, OH radicals were expected to be the main oxidant due to the fast reaction

214   rate constant of eugenol toward OH radicals obtained in this work. The decrease of

215   SOA yield at high OH exposure is possibly contributed from the C−C bond scission of

216   gas-phase species by further oxidation or heterogeneous reactions involving OH

217   radicals, which would generate a large amount of fragmented molecules that could not

218   condense on aerosol particles (Lambe et al., 2015; Ortega et al., 2016; Simonen et al.,

219   2017).

220   SOA yield can be described using a widely-used semi-empirical model on the basis

221   of the absorptive gas-particle partitioning of semi-volatile products, in which the overall

222   SOA yield (Y) is given by (Odum et al., 1996):

223 $$Y = \sum_i M_0 \frac{\alpha_i K_{om,i}}{1 + K_{om,i} M_0} \qquad (2)$$

224 where α_i is the mass-based stoichiometric coefficient for the reaction producing the

225 semi-volatile product i, $K_{om,i}$ is the gas-particle partitioning equilibrium constant, and

226 M_0 is the total aerosol mass concentration.

227 The SOA yield data in Table 2 can be plotted in the form of Eq. (2) to obtain the

228 yield curve for eugenol (Fig. 2). The simulation of experimental data indicated that an

229 one-product model could accurately reproduce the data ($R^2 = 0.98$), while the use of

230 two or more products in the model did not significantly improve the fitting quality.

231 Odum et al. (1996) reported that the SOA yield data from the oxidation of aromatic

232 compounds could be fitted well using a two-product model. However, an one-product

233 model was also efficient for describing the SOA yields from the oxidation of aromatics

234 including methoxyphenols (Lauraguais et al., 2012, 2014b; Coeur-Tourneur et al.,

235 2010b). The success of simulation with an one-product model in this work is likely to

236 indicate that the products in SOA have similar values of α_i and $K_{om,i}$, i.e., that the

237 obtained α_i (0.36 ±0.02) and $K_{om,i}$ (0.013 ±0.002 m^3 ug^{-1}) represent the average values.

238 In this work, considering that the composition of SOA was not determined, the volatility

239 basis set (VBS) approach was not applied to simulate SOA yields. Fig. S5 shows a plot

240 of the SOA mass concentration (M_0) versus the reacted eugenol concentration

241 (Δ[eugenol]). Its slope was 0.37 as obtained using linear least-squares fitting, which is

242 very close to the α_i value (0.36). This suggests that the low-volatility products formed

243 in the reaction almost completely disperse on the particle phase according to the

Atmospheric
Chemistry
and Physics
Discussions
Open Access
EGU

244   theoretical partition model (Lauraguais et al., 2012, 2014b). In other words, SOA yield

245   was approximately an upper limit for eugenol oxidation in the OFR. In view of the

246   residence time in this work, it seems be in contradiction with the recommendation of

247   longer residence time made by Ahlberg et al. (2017), who found that the condensation

248   of low-volatility species on SOA in the OFR was often kinetically limited at low mass

249   concentrations. In our recent experiments (not published), the SOA yields for guaiacol

250   oxidation by OH radicals obtained under the similar experimental conditions as this

251   work, could be comparable to those obtained in the chamber studies (Fig. S6). This

252   suggests that the effect of kinetic limitations on SOA condensation for the OH-initiated

253   oxidation of methoxyphenols in this system might be not important.

254   Elemental ratios (H/C and O/C) could provide insights into SOA composition and

255   chemical processes along with aging (Bruns et al., 2015). As shown in Fig. 3, O/C ratio

256   of SOA increases and H/C ratio decreases with increasing OH exposure, because

257   oxygen-containing functional groups are formed in the oxidation products. In addition,

258   the organic mass fractions of m/z 44 (CO_2^+) and m/z 43 (mostly $C_2H_3O^+$), named f_{44}

259   and f_{43}, respectively, could also provide information about the nature of SOA formation.

260   Fig. S7 shows the evolution of f_{44} and f_{43} versus OH exposure at low (272 μg m^{-3}) and

261   high (1328 μg m^{-3}) concentrations of eugenol. The values of f_{44} were much higher than

262   those of f_{43}, and increased significantly as a function of OH exposure, suggesting that

263   SOA formed in the experiments became more oxidized. The f_{44} value in this work

264   ranges up to 0.26, which is consistent with that observed for ambient low-volatility (LV-

265   OA), higher than 0.25 (Ng et al., 2010).

266   The average carbon oxidation state (OS_C) proposed by Kroll et al. (2011) is

267   considered a more accurate indicator of the oxidation degree of atmospheric organic

268   species than the O/C ratio alone, because it takes into account the saturation level of the

269   carbon atoms in the SOA. OS_C is defined as $OS_C = 2O/C - H/C$ (Kroll et al., 2011),

270   calculated according to the elemental composition of SOA measured by HR-ToF-AMS.

271   In this work, the OS_C values obtained at low (272 μg m^{-3}) and high (1328 μg m^{-3})

272   concentrations of eugenol were compared. As shown in Fig. 3, OS_C values for low

273   concentration (0.035−1.78) were much larger than those for high concentration

274   (0.0036−1.09), and increased linearly ($R^2 > 0.96$) with OH exposure of (1.21−12.55) ×

275   10^{11} molecules cm^{-3} s. The results are well supported by the evolution of SOA mass

276   spectra obtained by HR-ToF-AMS at the same eugenol concentrations (Fig. S8).

277   Similar trends have been observed in the smog chamber and PAM reactor (Simonen et

278   al., 2017; Ortega et al., 2016). The OS_C value in this work extends as high as 1.78,

279   which is in good agreement with that observed for ambient LV-OA, up to 1.9 (Kroll et

280   al., 2011). Recently, Ortega et al. (2016) reported that the OS_C value for SOA formed

281   from ambient air in an OFR ranged up to 2.0; and Simonen et al. (2017) determined a

282   high OS_C value (> 1.1) for SOA formed from the OH-initiated reaction of toluene in a

283   PAM reactor with an OH exposure of 1.2×10^{12} molecules cm^{-3} s. In general, the OS_C

284   values for the PAM reactor are higher than those for smog chambers due to the high

285   OH exposure in the PAM reactor (Simonen et al., 2017; Ortega et al., 2016; Lambe et

Atmospheric
Chemistry
and Physics
Discussions

286 al., 2015). Higher OS_C value indicates greater age, where the SOA components are

287 further oxidized through heterogeneous oxidation, adding substantial oxygen and

288 reducing hydrogen in the molecules in the particle-phase to increase OS_C values despite

289 the overall loss of SOA mass (Ortega et al., 2016).

290 **3.3 Effect of SO_2 on SOA formation**

291 As shown in Fig. 4, the presence of SO_2 favored SOA formation, and the sulfate

292 concentration increased linearly ($R^2 = 0.99$) as a function of OH exposure. The

293 maximum SOA yield enhancement of 38.57% was obtained at OH exposure of $5.41 \times$

294 10^{11} molecules cm^{-3} s, and then decreased with the increase of OH exposure due to the

295 fragmented molecules formed through the oxidation of gas-phase species by high OH

296 exposure (Lambe et al., 2015; Ortega et al., 2016; Simonen et al., 2017). The SOA yield

297 and sulfate concentration both increased linearly ($R^2 > 0.97$) as SO_2 concentration

298 increased from 0 to 198 ppbv at OH exposure of 1.21×10^{11} molecules cm^{-3} s (Fig. S9).

299 Compared to the initial SOA yield (0.049) obtained in the absence of SO_2, the SOA

300 yield (0.066) obtained in the presence of 198 ppbv SO_2 was enhanced by 34.69%. In

301 previous studies, Kleindienst et al. (2006) reported that the SOA yield from α-pinene

302 photooxidation increased by 40% in the presence of 252 ppbv SO_2; Liu et al. (2016b)

303 recently found that the SOA yield from 5 h photochemical aging of gasoline vehicle

304 exhaust was enhanced by 60−200% in the presence of ~150 ppbv SO_2.

305 As shown in Figs. 4 and S7, the increase of sulfate concentration was favorable for

306 SOA formation. In this system, it is difficult to completely remove trace NH_3, thus the

Atmospheric
Chemistry
and Physics
Discussions

307   formed sulfate was the mixture of sulfuric acid (H_2SO_4) and a small amount of

308   ammonium sulfate ((NH_4)$_2SO_4$). The in situ particle acidity was calculated as the H^+

309   concentration ([H^+], 40.23−648.39 nmol m^{-3}) according to the AIM-II model for the H−

310    $NH_4^+ - SO_4^{2-} - NO_3^- - H_2O$ systems (http://www.aim.env.uea.ac.uk/aim/model2 /model2

311   a.php; Liu et al., 2016b). The detailed description of the calculation method has been

312   represented elsewhere (Liu et al., 2016b). The elevated concentration of sulfate in the

313   particle phase with the increases of SO_2 concentration and OH exposure is an important

314   reason for the enhanced SOA yields (Kleindienst et al., 2006; Liu et al., 2016b). Cao

315   and Jang (2007) indicated that SOA yields from the oxidation of toluene and 1,3,5-

316   trimethylbenzene increased by 14−36% in the presence of acid seeds, with [H^+] of

317   240−860 nmol m^{-3} compared to those obtained in the presence of nonacid seeds. Similar

318   results concerning the effect of particle acidity on SOA yields were reported in other

319   studies (Kleindienst et al., 2006; Liu et al., 2016b; Jaoui et al., 2008; Xu et al., 2016).

320   However, Ng et al. (2007b) found that particle acidity had a negligible effect on SOA

321   yields from photooxidation of aromatics, possibly due to the low RH (~5%) used in

322   their work. The water content of aerosol plays an essential role in acidity effects (Cao

323   and Jang, 2007). Under acidic conditions, the gas-phase oxidation products of eugenol

324   would be partitioned more quickly into the particle-phase and further oxidized into low

325   volatility products, or produce oligomeric organics by acid-catalyzed heterogeneous

326   reactions, subsequently enhancing SOA yields (Cao and Jang, 2007; Jaoui et al., 2008;

327   Liu et al., 2016b; Xu et al., 2016). In addition, the formed sulfate not only serves as the

Atmospheric
Chemistry
and Physics
Discussions

328   substrate for product condensation and likely participates in new particle formation

329   (NPF) (Jaoui et al., 2008; Wang et al., 2016), but also enhances the surface areas of

330   particles to facilitate heterogeneous reactions on aerosols (Xu et al., 2016). These roles

331   of sulfate are also favorable for increasing SOA yields. Recently, Friedman et al. (2016)

332   have indicated that SO_2 could participate in the oxidation reactions of α-and β-pinene

333   and perturbs their oxidation in the OFR, but this possible effect could be ignored in this

334   work due to the relatively high RH and the negligible S/C ratio observed by HR-ToF-

335   AMS (Friedman et al., 2016).

336   **3.4   Effect of NO_2 on SOA formation**

337   It is well known that high NO_x concentration almost always plays a negative role in

338   NPF and SOA formation because the reaction of NO with RO_2 radicals results in the

339   formation of more volatile products compared to the reaction of HO_2 with RO_2 radicals

340   (Sarrafzadeh et al., 2016). Previous studies reported that nitro-substituted products were

341   the main products for SOA formed from OH-initiated reactions of phenol precursors

342   including methoxyphenols, in the presence of NO_x (Finewax et al., 2018; Ahmad et al.,

343   2017; Lauraguais et al., 2012, 2014b). Thus, the effect of NO_2 on SOA formation from

344   eugenol oxidation by OH radicals was investigated. As shown in Fig. 5, the nitrate

345   concentration measured by HR-ToF-AMS increased as a function of OH exposure in

346   the presence of 40 ppbv NO_2, but it was much lower than the sulfate concentration (Fig.

347   4) even though the OH rate constant for NO_2 was faster than that for SO_2 (Davis et al.,

348   1979; Atkinson et al., 1976). The possible explanation is that the formed HNO_3 mainly

Atmospheric
Chemistry
and Physics
Discussions

349   exists in the gas phase, and the relatively high temperature (301 $\pm$ 1 K) is not favorable

350   for gaseous HNO_3 distribution in the particle phase (Wang et al., 2016). It has been

351   indicated that the temperature range for the greatest loss of nitrate is 293−298 K (Keck

352   and Wittmaack, 2005). As illustrated in Fig. 5, the SOA yield enhancement and N/C

353   ratio both increased firstly and then decreased with rising OH exposure. The increase

354   of NO_2 concentration (40−109 ppbv) is beneficial to SOA yields (0.053−0.062), N/C

355   ratio (0.032−0.041), and nitrate formation (4.29−6.30 µg m^{-3}) (Fig. S10). Compared to

356   the presence of 41 ppbv SO_2, the maximum SOA yield enhancement (19.17%) in the

357   presence of 40 ppbv NO_2 is lower. For most aromatic precursors, the addition of ppbv

358   levels of NO_2 should have a negligible effect on SOA formation, because the rate

359   constants of OH-aromatic adducts with O_2 and NO_2 are on the order of approximate 10^{-16}

360   and 10^{-11} cm^3 molecule^{-1} s^{-1}, respectively (Atkinson and Arey, 2003). But, for phenol

361   precursors only about 0.5 ppbv NO_2 is enough to compete with O_2 for the reaction with

362   OH-aromatic adducts (Finewax et al., 2018). Therefore, the enhancement effect of NO_2

363   on SOA formation might be relevant to the special case of phenols or methoxyphenols

364   but not other aromatic precursors.

365   It is noteworthy that the N/C ratio is in the range of 0.032−0.043, suggesting that

366   NO_2 participated in the OH reaction of eugenol, through the addition to the OH-eugenol

367   adduct (Peng and Jimenez, 2017). Recently, Hunter et al. (2014) found that NO_2

368   participated in the OH reactions of yclic alkanes, and the N/C ratios were in the range

369   of 0.031−0.064, higher than those obtained in this work. The nitro-substituted products

Atmospheric
Chemistry
and Physics
Discussions

370   are reported to be the main reaction products of the OH reactions of guaiacol and

371   syringol in the presence of NO_2 (Lauraguais et al., 2014b; Ahmad et al., 2017). The N-

372   containing products might be also formed through the reactions involving with NO_3

373   radicals, which are possibly generated by the reaction between NO_2 and O_3 in this

374   system (Atkinson, 1991). But, the specific contribution of NO_3 radicals could not be

375   quantified in this work. The relative low volatility of these products could reasonably

376   contribute to SOA formation (Duporté et al., 2016; Liu et al., 2016a). In addition, higher

377   NO_2/NO ratio favors the formation of nitro-substituted products, which are potentially

378   involved in NPF and SOA growth (Pereira et al., 2015). Ng et al. (2007a) also indicated

379   that NO_x could be beneficial to SOA formation for sesquiterpenes, due to the formation

380   of low volatility organic nitrates and the isomerization of large alkoxy radicals, resulting

381   in less volatile products. The decrease in the N/C ratio at high OH exposure suggested

382   that more volatile products were generated through the oxidation of particle-phase

383   species by OH radicasls.

384   The NO^+ / NO_2^+ ratios measured by HR-ToF-MS are widely used to identify

385   inorganic and organic nitrates. The NO^+ / NO_2^+ ratios for inorganic nitrates have been

386   reported to be in the range of 1.08−2.81 (Farmer et al., 2010; Sato et al., 2010). The

387   ratio ranged from 2.06 to 2.54 in this work as determined by HR-ToF-AMS using

388   ammonium nitrate as the calibration sample. However, the NO^+ / NO_2^+ ratios during

389   oxidation of eugenol in the presence of 40 ppbv NO_2 were 3.98−6.09. They were higher

390   than those for inorganic nitrates and consistent with those for organic nitrates

391 (3.82−5.84) from the photooxidation of aromatics (Sato et al., 2010). The abundance of

392 organic nitrates could be estimated from the N/C ratios determined in this work.

393 Assuming that the oxidation products in the SOA retain 10 carbon atoms, the yields of

394 organic nitrates are in the range of 32−43%, which are comparable to those reported in

395 earlier studies (Liu et al., 2015; Hunter et al., 2014). Liu et al. (2015) reported that the

396 nitrogen-containing organic mass contributed $31.5 \pm 4.4\%$ to the total SOA derived

397 from m-xylene oxidation by OH radicals. Hunter et al. (2014) estimated the organic

398 nitrate yields of SOA to be 31−64%, formed in the OH-initiated reactions of acyclic,

399 monocyclic, and polycyclic alkanes. This range obtained in this work should be the

400 upper limit due to the possibility of C−C bond scission of gas- and particle-phase

401 organics oxidized by high OH exposure. Besides, the maximum yield of nitrates for a

402 single reaction step is expected to be approximately 30% (Ziemann and Atkinson, 2012),

403 this suggests that multiple reaction steps are needed.

404 **3.5 Atmospheric implications**

405 Biomass burning not only serves as a major contributor of atmospheric POA, but also

406 has great SOA formation potential through atmospheric oxidation (Bruns et al., 2016;

407 Gilardoni et al., 2016; Li et al., 2017; Ciarelli et al., 2017; Ding et al., 2017). Recent

408 studies have indicated that SOA formed from biomass burning plays an important role

409 in haze pollution in China (Li et al., 2017; Ding et al., 2017). Residential combustion

410 (mainly wood burning) could contribute approximately 60−70% to SOA formation in

411 winter at the European scale (Ciarelli et al., 2017). In addition, methoxyphenols are the

Atmospheric
Chemistry
and Physics
Discussions

412   major component of OA from biomass burning (Bruns et al., 2016; Schauer and Cass,

413   2000). Based on our results and those of previous studies (Sun et al., 2010; Lauraguais

414   et al., 2012, 2014b; Ahmad et al., 2017; Yee et al., 2013; Ofner et al., 2011), it should

415   pay more attenion on the SOA formation from the OH oxidation of biomass burning

416   emissions and its subsequent effect on haze evolution, especially in China with

417   nationwide biomass burning and high daytime average [OH] in the ambient atmosphere

418    $((5.2-7.5) \times 10^6$ molecules cm^{-3}) (Yang et al., 2017). Meanwhile, the potential

419   contributions of SO_2 and NO_2 to SOA formation should also be taken into account,

420   because the concentrations of NO_x and SO_2 could be up to close 200 ppbv in the

421   severely polluted atmosphere in China (Li et al., 2017). Although eugenol

422   concentrations in this work are higher than those in the ambient atmosphere, the results

423   obtained in this work could provide new information for SOA formation from the

424   atmospheric oxidation of methoxyphenols, and might be useful for SOA modeling,

425   especially for air quality simulation modeling of the specific regions experiencing

426   serious pollution caused by fine particulate matter.

427   N-containing products formed from the oxidation of methoxyphenols could

428   contribute to water-soluble organics in SOA (Lauraguais et al., 2014b; Yang et al., 2016;

429   Zhang et al., 2016), which have been widely detected in atmospheric humic-like

430   substances (HULIS) (Wang et al., 2017). Due to their surface-active and UV-light-

431   absorbing properties, HULIS could influence the formation of cloud condensation

432   nuclei (CCN), solar radiation balance, and photochemical processes in the atmosphere

Atmospheric
Chemistry
and Physics
Discussions

433 (Wang et al., 2017). The high reactivity of methoxyphenols toward atmospheric radicals

434 suggests that SOA was formed from their oxidation processes with relatively high

435 oxidation level, subsequently leading to SOA with strong optical absorption and

436 hygroscopic properties (Lambe et al., 2013; Massoli et al., 2010). Therefore, SOA

437 formed from the reactions of methoxyphenols with atmospheric oxidants might have

438 important effects on air quality and climate. In addition, the experimental results from

439 this study would help to further the understanding of the atmospheric aging process of

440 smoke plumes from biomass-burning emissions.

441 **4   Conclusions**

442 For the first time, the rate constant and SOA foramtion for the gas-phase reaction of

443 eugenol with OH radicals were investigated in an OFR. The second-order rate constant

444 of eugenol with OH radicals was $(8.01 \pm 0.40) \times 10^{-11}$ cm^3 molecule^{-1} s^{-1}, measured by

445 the relative rate method, and the corresponding atmospheric lifetime was 2.31 h. In

446 addition, the significant SOA formation of eugenol oxidation by OH radicals was

447 observed. The maximum SOA yields (0.11−0.31) obtained at different eugenol

448 concentrations could be expressed well by an one-product model. SOA yield was

449 dependent on OH exposure and eugenol concentration, which firstly increased and then

450 decreased as a function of OH exposure due to the possible C−C bond scission of gas-

451 phase species by further oxidation or heterogeneous reactions involving OH radicals.

452 The OS_C and O/C ratio both increased significantly as a function of OH exposure,

453 suggesting that SOA became more oxidized. The presence of SO_2 and NO_2 was helpful

Atmospheric
Chemistry
and Physics
Discussions

454   to increase SOA yield, and the maximum enhanced yields were 38.57% and 19.17%,

455   respectively. The observed N/C ratio of SOA was in the range of 0.032−0.043,

456   indicating that NO_2 participated in the OH-initiated reaction of eugenol, consequently

457   producing organic nitrates. The experimental results might be helpful to further

458   understand the atmospheric chemical behavior of eugenol and its SOA formation

459   potential from OH oxidation in the atmosphere.

460   **Data availability**

461   The experimental data are available upon request to the corresponding authors.

462   **Competing interests**

463   The authors declare that they have no conflict of interest.

Atmospheric
Chemistry
and Physics
Discussions

References

474   Ahlberg, E., Falk, J., Eriksson, A., Holst, T., Brune, W. H., Kristensson, A., Roldin, P.,
475   and Svenningsson, B.: Secondary organic aerosol from VOC mixtures in an
476   oxidation   flow   reactor,   Atmos.   Environ.,   161,   210-220,   doi:
477   10.1016/j.atmosenv.2017.05.005, 2017.
478   Ahmad, W., Coeur, C., Tomas, A., Fagniez, T., Brubach, J.-B., and Cuisset, A.: Infrared
479   spectroscopy of secondary organic aerosol precursors and investigation of the
480   hygroscopicity of SOA formed from the OH reaction with guaiacol and syringol,
481   Appl. Opt., 56, E116-E122, doi: 10.1364/ao.56.00e116, 2017.
482   Atkinson, R., Perry, R. A., and Pitts, J. N.: Rate constants for the reactions of the OH
483   radicals with NO_2 (M = Ar and N_2) and SO_2 (M = Ar), J. Chem. Phys., 65, 306-
484   310, doi: 10.1063/1.432770, 1976.
485   Atkinson, R.: Kinetics and mechanisms of the gas-phase reactions of the NO_3 radical
486   with organic compounds, J. Phys. Chem. Ref. Data, 20, 459-507, doi:
487   10.1063/1.555887, 1991.
488   Atkinson, R., and Arey, J.: Atmospheric degradation of volatile organic compounds,
489   Chem. Rev., 103, 4605-4638, doi: 10.1021/cr0206420, 2003.
490   Bari, M. A., Baumbach, G., Kuch, B., and Scheffknecht, G.: Wood smoke as a source
491   of particle-phase organic compounds in residential areas, Atmos. Environ., 43,
492   4722-4732, doi: 10.1016/j.atmosenv.2008.09.006, 2009.
493   Bari, M. A., Baumbach, G., Kuch, B., and Scheffknecht, G.: Temporal variation and
494   impact of wood smoke pollution on a residential area in southern Germany, Atmos.
495   Environ., 44, 3823-3832, doi: 10.1016/j.atmosenv.2010.06.031, 2010.
496   Bolling, A. K., Pagels, J., Yttri, K. E., Barregard, L., Sallsten, G., Schwarze, P. E., and
497   Boman, C.: Health effects of residential wood smoke particles: the importance of
498   combustion conditions and physicochemical particle properties, Part. Fibre
499   Toxicol., 6, doi: 10.1186/1743-8977-6-29, 2009.
500   Bruns, E. A., El Haddad, I., Keller, A., Klein, F., Kumar, N. K., Pieber, S. M., Corbin,
501   J. C., Slowik, J. G., Brune, W. H., Baltensperger, U., and Prevot, A. S. H.: Inter-
502   comparison of laboratory smog chamber and flow reactor systems on organic
503   aerosol yield and composition, Atmos. Meas. Tech., 8, 2315-2332, doi:
504   10.5194/amt-8-2315-2015, 2015.
505   Bruns, E. A., El Haddad, I., Slowik, J. G., Kilic, D., Klein, F., Baltensperger, U., and
506   Prevot, A. S. H.: Identification of significant precursor gases of secondary organic
507   aerosols from residential wood combustion, Sci. Rep., 6., doi: 10.1038/srep27881,
508   2016.
509   Cao, G., and Jang, M.: Effects of particle acidity and UV light on secondary organic
510   aerosol formation from oxidation of aromatics in the absence of NO_x, Atmos.
511   Environ., 41, 7603-7613, doi: 10.1016/j.atmosenv.2007.05.034, 2007.
512   Chen, Y., and Bond, T. C.: Light absorption by organic carbon from wood combustion,
513   Atmos. Chem. Phys., 10, 1773-1787, doi: 10.5194/acp-10-1773-2010, 2010.

Atmospheric
Chemistry
and Physics
Discussions

514 Ciarelli, G., Aksoyoglu, S., El Haddad, I., Bruns, E. A., Crippa, M., Poulain, L., Aijala,
515   M., Carbone, S., Freney, E., O'Dowd, C., Baltensperger, U., and Prevot, A. S. H.:
516   Modelling winter organic aerosol at the European scale with CAMx: Evaluation
517   and source apportionment with a VBS parameterization based on novel wood
518   burning smog chamber experiments, Atmos. Chem. Phys., 7, 7653-7669, doi:
519   10.5194/acp-17-7653-2017, 2017.
520 Coeur-Tourneur, C., Cassez, A., and Wenger, J. C.: Rate Coefficients for the gas-phase
521   reaction of hydroxyl radicals with 2-methoxyphenol (guaiacol) and related
522   compounds, J. Phys. Chem. A, 114, 11645-11650, doi: 10.1021/jp1071023, 2010a.
523 Coeur-Tourneur, C., Foulon, V., and Lareal, M.: Determination of aerosol yields from
524   3-methylcatechol and 4-methylcatechol ozonolysis in a simulation chamber,
525   Atmos. Environ., 44, 852-857, doi: 10.1016/j.atmosenv.2009.11.027, 2010b.
526 Davis, D. D., Ravishankara, A. R., and Fischer, S.: SO_2 oxidation via the hydroxyl
527   radical: Atmospheric fate of HSO_x radicals, Geophys. Res. Lett., 6, 113-116, doi:
528   10.1029/GL006i002p00113, 1979.
529 DeCarlo, P. F., Slowik, J. G., Worsnop, D. R., Davidovits, P., and Jimenez, J. L.: Particle
530   morphology and density characterization by combined mobility and aerodynamic
531   diameter measurements. Part 1: Theory, Aerosol Sci. Technol., 38, 1185-1205, doi:
532   10.1080/027868290903907, 2004.
533 DeCarlo, P. F., Kimmel, J. R., Trimborn, A., Northway, M. J., Jayne, J. T., Aiken, A. C.,
534   Gonin, M., Fuhrer, K., Horvath, T., Docherty, K. S., Worsnop, D. R., and Jimenez,
535   J. L.: Field-deployable, high-resolution, time-of-flight aerosol mass spectrometer,
536   Anal. Chem., 78, 8281-8289, doi: 10.1021/ac061249n, 2006.
537 Dills, R. L., Paulsen, M., Ahmad, J., Kalman, D. A., Elias, F. N., and Simpson, C. D.:
538   Evaluation of urinary methoxyphenols as biomarkers of woodsmoke exposure,
539   Environ. Sci. Technol., 40, 2163-2170, doi: 10.1021/es051886f, 2006.
540 Ding, X., Zhang, Y.-Q., He, Q.-F., Yu, Q.-Q., Wang, J.-Q., Shen, R.-Q., Song, W., Wang,
541   Y.-S., and Wang, X.-M.: Significant increase of aromatics-derived secondary
542   organic aerosol during fall to winter in China, Environ. Sci. Technol., 51, 7432-
543   7441, doi: 10.1021/acs.est.6b06408, 2017.
544 Duporté, G., Parshintsev, J., Barreira, L. M. F., Hartonen, K., Kulmala, M., and
545   Riekkola, M.-L.: Nitrogen-containing low volatile compounds from
546   pinonaldehyde-dimethylamine reaction in the atmosphere: A laboratory and field
547   study, Environ. Sci. Technol., 50, 4693-4700, doi: 10.1021/acs.est.6b00270, 2016.
548 El Zein, A., Coeur, C., Obeid, E., Lauraguais, A., and Fagniez, T.: Reaction kinetics of
549   catechol (1,2-benzenediol) and guaiacol (2-methoxyphenol) with ozone, J. Phys.
550   Chem. A, 119, 6759-6765, doi: 10.1021/acs.jpca.5b00174, 2015.
551 Farmer, D. K., Matsunaga, A., Docherty, K. S., Surratt, J. D., Seinfeld, J. H., Ziemann,
552   P. J., and Jimenez, J. L.: Response of an aerosol mass spectrometer to
553   organonitrates and organosulfates and implications for atmospheric chemistry,
554   Proc. Natl. Acad. Sci. U. S. A, 107, 6670-6675, doi: 10.1073/pnas.0912340107,
555   2010.

556 Finewax, Z., de Gouw, J. A., and Ziemann, P. J.: Identification and quantification of 4-
557   nitrocatechol formed from OH and NO_3 radical-initiated reactions of catechol in
558   air in the presence of NO_x: Implications for secondary organic aerosol formation
559   from biomass burning, Environ. Sci. Technol., 52, 1981-1989, doi:
560   10.1021/acs.est.7b05864, 2018.
561 Friedman, B., Brophy, P., Brune, W. H., and Farmer, D. K.: Anthropogenic sulfur
562   perturbations on biogenic oxidation: SO_2 additions impact gas-phase OH oxidation
563   products of alpha- and beta-pinene, Environ. Sci. Technol., 50, 1269-1279, doi:
564   10.1021/acs.est.5b05010, 2016.
565 Gilardoni, S., Massoli, P., Paglione, M., Giulianelli, L., Carbone, C., Rinaldi, M.,
566   Decesari, S., Sandrini, S., Costabile, F., Gobbi, G. P., Pietrogrande, M. C., Visentin,
567   M., Scotto, F., Fuzzi, S., and Facchini, M. C.: Direct observation of aqueous
568   secondary organic aerosol from biomass-burning emissions, Proc. Natl. Acad. Sci.
569   U. S. A, 113, 10013-10018, doi: 10.1073/pnas.1602212113, 2016.
570 Gordon, T. D., Presto, A. A., Nguyen, N. T., Robertson, W. H., Na, K., Sahay, K. N.,
571   Zhang, M., Maddox, C., Rieger, P., Chattopadhyay, S., Maldonado, H., Maricq, M.
572   M., and Robinson, A. L.: Secondary organic aerosol production from diesel
573   vehicle exhaust: impact of aftertreatment, fuel chemistry and driving cycle, Atmos.
574   Chem. Phys., 14, 4643-4659, doi: 10.5194/acp-14-4643-2014, 2014.
575 http://www.aim.env.uea.ac.uk/aim/model2/model2a.php.
576 Hunter, J. F., Carrasquillo, A. J., Daumit, K. E., and Kroll, J. H.: Secondary organic
577   aerosol formation from acyclic, monocyclic, and polycyclic alkanes, Environ. Sci.
578   Technol., 48, 10227-10234, doi: 10.1021/es502674s, 2014.
579 Jaoui, M., Edney, E. O., Kleindienst, T. E., Lewandowski, M., Offenberg, J. H., Surratt,
580   J. D., and Seinfeld, J. H.: Formation of secondary organic aerosol from irradiated
581   alpha-pinene/toluene/NO_x mixtures and the effect of isoprene and sulfur dioxide,
582   J. Geophys. Res.-Atmos., 113, doi: 10.1029/2007jd009426, 2008.
583 Jeong, C.-H., Evans, G. J., Dann, T., Graham, M., Herod, D., Dabek-Zlotorzynska, E.,
584   Mathieu, D., Ding, L., and Wang, D.: Influence of biomass burning on wintertime
585   fine particulate matter: Source contribution at a valley site in rural British
586   Columbia, Atmos. Environ., 42, 3684-3699, doi: 10.1016/j.atmosenv.2008.01.006,
587   2008.
588 Kang, E., Root, M. J., Toohey, D. W., and Brune, W. H.: Introducing the concept of
589   Potential Aerosol Mass (PAM), Atmos. Chem. Phys., 7, 5727-5744, doi:
590   10.5194/acp-7-5727-2007, 2007.
591 Keck, L., and Wittmaack, K.: Effect of filter type and temperature on volatilisation
592   losses from ammonium salts in aerosol matter, Atmos. Environ., 39, 4093-4100,
593   doi: 10.1016/j.atmosenv.2005.03.029, 2005.
594 Kleindienst, T. E., Shepson, P. B., Edney, E. O., Claxton, L. D., and Cupitt, L. T.: Wood
595   smoke: Measurement of the mutagenic activities of its gas- and particulate-phase
596   photooxidation products, Environ. Sci. Technol., 20, 493-501, doi:
597   10.1021/es00147a009, 1986.

Atmospheric
Chemistry
and Physics
Discussions

598 Kleindienst, T. E., Edney, E. O., Lewandowski, M., Offenberg, J. H., and Jaoui, M.:
599   Secondary organic carbon and aerosol yields from the irradiations of isoprene and
600   alpha-pinene in the presence of NO_x and SO_2, Environ. Sci. Technol., 40, 3807-
601   3812, doi: 10.1021/es052446r, 2006.
602 Kramp, F., and Paulson, S. E.: On the uncertainties in the rate coefficients for OH
603   reactions with hydrocarbons, and the rate coefficients of the 1,3,5-
604   trimethylbenzene and m-xylene reactions with OH radicals in the gas phase, J.
605   Phys. Chem. A, 102, 2685-2690, doi: 10.1021/jp973289o, 1998.
606 Kroll, J. H., Donahue, N. M., Jimenez, J. L., Kessler, S. H., Canagaratna, M. R., Wilson,
607   K. R., Altieri, K. E., Mazzoleni, L. R., Wozniak, A. S., Bluhm, H., Mysak, E. R.,
608   Smith, J. D., Kolb, C. E., and Worsnop, D. R.: Carbon oxidation state as a metric
609   for describing the chemistry of atmospheric organic aerosol, Nature Chem., 3, 133-
610   139, doi: 10.1038/nchem.948, 2011.
611 Lambe, A. T., Cappa, C. D., Massoli, P., Onasch, T. B., Forestieri, S. D., Martin, A. T.,
612   Cummings, M. J., Croasdale, D. R., Brune, W. H., Worsnop, D. R., and Davidovits,
613   P.: Relationship between oxidation level and optical properties of secondary
614   organic aerosol, Environ. Sci. Technol., 47, 6349-6357, doi: 10.1021/es401043j,
615   2013.
616 Lambe, A. T., Chhabra, P. S., Onasch, T. B., Brune, W. H., Hunter, J. F., Kroll, J. H.,
617   Cummings, M. J., Brogan, J. F., Parmar, Y., Worsnop, D. R., Kolb, C. E., and
618   Davidovits, P.: Effect of oxidant concentration, exposure time, and seed particles
619   on secondary organic aerosol chemical composition and yield, Atmos. Chem.
620   Phys., 15, 3063-3075, doi: 10.5194/acp-15-3063-2015, 2015.
621 Lauraguais, A., Coeur-Tourneur, C., Cassez, A., and Seydi, A.: Rate constant and
622   secondary organic aerosol yields for the gas-phase reaction of hydroxyl radicals
623   with syringol (2,6-dimethoxyphenol), Atmos. Environ., 55, 43-48, doi:
624   10.1016/j.atmosenv.2012.02.027, 2012.
625 Lauraguais, A., Bejan, I., Barnes, I., Wiesen, P., Coeur-Tourneur, C., and Cassez, A.:
626   Rate coefficients for the gas-phase reaction of chlorine atoms with a series of
627   methoxylated aromatic compounds, J. Phys. Chem. A, 118, 1777-1784, doi:
628   10.1021/jp4114877, 2014a.
629 Lauraguais, A., Coeur-Tourneur, C., Cassez, A., Deboudt, K., Fourmentin, M., and
630   Choel, M.: Atmospheric reactivity of hydroxyl radicals with guaiacol (2-
631   methoxyphenol), a biomass burning emitted compound: Secondary organic
632   aerosol formation and gas-phase oxidation products, Atmos. Environ., 86, 155-
633   163, doi: 10.1016/j.atmosenv.2013.11.074, 2014b.
634 Lauraguais, A., Bejan, I, Barnes, I., Wiesen, P., and Coeur, C.: Rate coefficients for the
635   gas-phase reactions of hydroxyl radicals with a series of methoxylated aromatic
636   compounds, J. Phys. Chem. A, 119, 6179-6187, doi: 10.1021/acs.jpca.5b03232,
637   2015.
638 Lauraguais, A., El Zein, A., Coeur, C., Obeid, E., Cassez, A., Rayez, M.-T., and Rayez,
639   J.-C.: Kinetic study of the gas-phase reactions of nitrate radicals with

Atmospheric
Chemistry
and Physics
Discussions

640   methoxyphenol compounds: Experimental and theoretical approaches, J. Phys.
641   Chem. A, 120, 2691-2699, doi: 10.1021/acs.jpca.6b02729, 2016.

642 Li, H., Zhang, Q., Zhang, Q., Chen, C., Wang, L., Wei, Z., Zhou, S., Parworth, C.,
643   Zheng, B., Canonaco, F., Prevot, A. S. H., Chen, P., Zhang, H., Wallington, T. J.,
644   and He, K.: Wintertime aerosol chemistry and haze evolution in an extremely
645   polluted city of the North China Plain: Significant contribution from coal and
646   biomass combustion, Atmos. Chem. Phys., 17, 4751-4768, doi: 10.5194/acp-17-
647   4751-2017, 2017.

648 Li, R., Palm, B. B., Ortega, A. M., Hlywiak, J., Hu, W., Peng, Z., Day, D. A., Knote, C.,
649   Brune, W. H., de Gouw, J. A., and Jimenez, J. L.: Modeling the radical chemistry
650   in an oxidation flow reactor: Radical formation and recycling, sensitivities, and
651   the OH exposure estimation equation, J. Phys. Chem. A, 119, 4418-4432, doi:
652   10.1021/jp509534k, 2015.

653 Liu, J., Lin, P., Laskin, A., Laskin, J., Kathmann, S. M., Wise, M., Caylor, R., Imholt,
654   F., Selimovic, V., and Shilling, J. E.: Optical properties and aging of light-
655   absorbing secondary organic aerosol, Atmos. Chem. Phys., 16, 12815-12827, doi:
656   10.5194/acp-16-12815-2016, 2016a.

657 Liu, T., Wang, X., Hu, Q., Deng, W., Zhang, Y., Ding, X., Fu, X., Bernard, F., Zhang,
658   Z., Lu, S., He, Q., Bi, X., Chen, J., Sun, Y., Yu, J., Peng, P., Sheng, G., and Fu, J.:
659   Formation of secondary aerosols from gasoline vehicle exhaust when mixing with
660   SO_2, Atmos. Chem. Phys., 16, 675-689, doi: 10.5194/acp-16-675-2016, 2016b.

661 Liu, Y., Liggio, J., Harner, T., Jantunen, L., Shoeib, M., and Li, S.-M.: Heterogeneous
662   OH initiated oxidation: A possible explanation for the persistence of
663   organophosphate flame retardants in air, Environ. Sci. Technol., 48, 1041-1048,
664   doi: 10.1021/es404515k, 2014.

665 Liu, Y., Liggio, J., Staebler, R., and Li, S. M.: Reactive uptake of ammonia to secondary
666   organic aerosols: Kinetics of organonitrogen formation, Atmos. Chem. Phys., 15,
667   13569-13584, doi: 10.5194/acp-15-13569-2015, 2015.

668 Mao, J., Ren, X., Brune, W. H., Olson, J. R., Crawford, J. H., Fried, A., Huey, L. G.,
669   Cohen, R. C., Heikes, B., Singh, H. B., Blake, D. R., Sachse, G. W., Diskin, G. S.,
670   Hall, S. R., and Shetter, R. E.: Airborne measurement of OH reactivity during
671   INTEX-B, Atmos. Chem. Phys., 9, 163-173, doi: 10.5194/acp-9-163-2009, 2009.

672 Massoli, P., Lambe, A. T., Ahern, A. T., Williams, L. R., Ehn, M., Mikkila, J.,
673   Canagaratna, M. R., Brune, W. H., Onasch, T. B., Jayne, J. T., Petaja, T., Kulmala,
674   M., Laaksonen, A., Kolb, C. E., Davidovits, P., and Worsnop, D. R.: Relationship
675   between aerosol oxidation level and hygroscopic properties of laboratory
676   generated secondary organic aerosol (SOA) particles, Geophys. Res. Lett., 37, doi:
677   10.1029/2010gl045258, 2010.

678 McMurry, J. E.: Organic Chemistry, 6th ed., 2004.

679 Ng, N. L., Chhabra, P. S., Chan, A. W. H., Surratt, J. D., Kroll, J. H., Kwan, A. J.,
680   McCabe, D. C., Wennberg, P. O., Sorooshian, A., Murphy, S. M., Dalleska, N. F.,
681   Flagan, R. C., and Seinfeld, J. H.: Effect of NOx level on secondary organic

Atmospheric
Chemistry
and Physics
Discussions

682   aerosol (SOA) formation from the photooxidation of terpenes, Atmos. Chem.
683   Phys., 7, 5159-5174, doi: 10.5194/acp-7-5159-2007, 2007a.
684   Ng, N. L., Kroll, J. H., Chan, A. W. H., Chhabra, P. S., Flagan, R. C., and Seinfeld, J.
685   H.: Secondary organic aerosol formation from m-xylene, toluene, and benzene,
686   Atmos. Chem. Phys., 7, 3909-3922, doi: 10.5194/acp-7-3909-2007, 2007b.
687   Ng, N. L., Canagaratna, M. R., Zhang, Q., Jimenez, J. L., Tian, J., Ulbrich, I. M., Kroll,
688   J. H., Docherty, K. S., Chhabra, P. S., Bahreini, R., Murphy, S. M., Seinfeld, J. H.,
689   Hildebrandt, L., Donahue, N. M., DeCarlo, P. F., Lanz, V. A., Prevot, A. S. H.,
690   Dinar, E., Rudich, Y., and Worsnop, D. R.: Organic aerosol components observed
691   in Northern Hemispheric datasets from Aerosol Mass Spectrometry, Atmos. Chem.
692   Phys., 10, 4625-4641, doi: 10.5194/acp-10-4625-2010, 2010.
693   Nolte, C. G., Schauer, J. J., Cass, G. R., and Simoneit, B. R. T.: Highly polar organic
694   compounds present in wood smoke and in the ambient atmosphere, Environ. Sci.
695   Technol., 35, 1912-1919, doi: 10.1021/es001420r, 2001.
696   Odum, J. R., Hoffmann, T., Bowman, F., Collins, D., Flagan, R. C., and Seinfeld, J. H.:
697   Gas/particle partitioning and secondary organic aerosol yields, Environ. Sci.
698   Technol., 30, 2580-2585, doi: 10.1021/es950943+, 1996.
699   Ofner, J., Krueger, H. U., Grothe, H., Schmitt-Kopplin, P., Whitmore, K., and Zetzsch,
700   C.: Physico-chemical characterization of SOA derived from catechol and guaiacol
701   - a model substance for the aromatic fraction of atmospheric HULIS, Atmos. Chem.
702   Phys., 11, 1-15, doi: 10.5194/acp-11-1-2011, 2011.
703   Ortega, A. M., Hayes, P. L., Peng, Z., Palm, B. B., Hu, W., Day, D. A., Li, R., Cubison,
704   M. J., Brune, W. H., Graus, M., Warneke, C., Gilman, J. B., Kuster, W. C., de
705   Gouw, J., Gutierrez-Montes, C., and Jimenez, J. L.: Real-time measurements of
706   secondary organic aerosol formation and aging from ambient air in an oxidation
707   flow reactor in the Los Angeles area, Atmos. Chem. Phys., 16, 7411-7433, doi:
708   10.5194/acp-16-7411-2016, 2016.
709   Peng, Z., Day, D. A., Stark, H., Li, R., Lee-Taylor, J., Palm, B. B., Brune, W. H., and
710   Jimenez, J. L.: HOx radical chemistry in oxidation flow reactors with low-pressure
711   mercury lamps systematically examined by modeling, Atmos. Meas. Tech., 8,
712   4863-4890, doi: 10.5194/amt-8-4863-2015, 2015.
713   Peng, Z., Day, D. A., Ortega, A. M., Palm, B. B., Hu, W., Stark, H., Li, R., Tsigaridis,
714   K., Brune, W. H., and Jimenez, J. L.: Non-OH chemistry in oxidation flow reactors
715   for the study of atmospheric chemistry systematically examined by modeling,
716   Atmos. Chem. Phys., 16, 4283-4305, doi: 10.5194/acp-16-4283-2016, 2016.
717   Peng, Z., and Jimenez, J. L.: Modeling of the chemistry in oxidation flow reactors with
718   high initial NO, Atmos. Chem. Phys., 17, 11991-12010, doi: 10.5194/acp-17-
719   11991-2017, 2017.
720   Pereira, K. L., Hamilton, J. F., Rickard, A. R., Bloss, W. J., Alam, M. S., Camredon, M.,
721   Ward, M. W., Wyche, K. P., Munoz, A., Vera, T., Vazquez, M., Borras, E., and
722   Rodenas, M.: Insights into the formation and evolution of individual compounds
723   in the particulate phase during aromatic photo-oxidation, Environ. Sci. Technol.,

Atmospheric
Chemistry
and Physics
Discussions

724   49, 13168-13178, doi: 10.1021/acs.est.5b03377, 2015.

725 Sarrafzadeh, M., Wildt, J., Pullinen, I., Springer, M., Kleist, E., Tillmann, R., Schmitt,
726   S. H., Wu, C., Mentel, T. F., Zhao, D., Hastie, D. R., and Kiendler-Scharr, A.:
727   Impact of NOx and OH on secondary organic aerosol formation from beta-pinene
728   photooxidation, Atmos. Chem. Phys., 16, 11237-11248, doi: 10.5194/acp-16-
729   11237-2016, 2016.

730 Sato, K., Takami, A., Isozaki, T., Hikida, T., Shimono, A., and Imamura, T.: Mass
731   spectrometric study of secondary organic aerosol formed from the photo-oxidation
732   of   aromatic   hydrocarbons,   Atmos.   Environ.,   44,   1080-1087,   doi:
733   10.1016/j.atmosenv.2009.12.013, 2010.

734 Schauer, J. J., and Cass, G. R.: Source apportionment of wintertime gas-phase and
735   particle-phase air pollutants using organic compounds as tracers, Environ. Sci.
736   Technol., 34, 1821-1832, doi: 10.1021/es981312t, 2000.

737 Schauer, J. J., Kleeman, M. J., Cass, G. R., and Simoneit, B. R. T.: Measurement of
738   emissions from air pollution sources. 3. C-1-C-29 organic compounds from
739   fireplace combustion of wood, Environ. Sci. Technol., 35, 1716-1728, doi:
740   10.1021/es001331e, 2001.

741 Simonen, P., Saukko, E., Karjalainen, P., Timonen, H., Bloss, M., Aakko-Saksa, P.,
742   Ronkko, T., Keskinen, J., and Dal Maso, M.: A new oxidation flow reactor for
743   measuring secondary aerosol formation of rapidly changing emission sources,
744   Atmos. Meas. Tech., 10, 1519-1537, doi: 10.5194/amt-10-1519-2017, 2017.

745 Simpson, C. D., Paulsen, M., Dills, R. L., Liu, L. J. S., and Kalman, D. A.:
746   Determination of methoxyphenols in ambient atmospheric particulate matter:
747   Tracers for wood combustion, Environ. Sci. Technol., 39, 631-637, doi:
748   10.1021/es0486871, 2005.

749 Sun, Y. L., Zhang, Q., Anastasio, C., and Sun, J.: Insights into secondary organic aerosol
750   formed via aqueous-phase reactions of phenolic compounds based on high
751   resolution mass spectrometry, Atmos. Chem. Phys., 10, 4809-4822, doi:
752   10.5194/acp-10-4809-2010, 2010.

753 Thuner, L. P., Bardini, P., Rea, G. J., and Wenger, J. C.: Kinetics of the gas-phase
754   reactions of OH and NO3 radicals with dimethylphenols, J. Phys. Chem. A, 108,
755   11019-11025, 10.1021/jp046358p, 2004.

756 Tiitta, P., Leskinen, A., Hao, L., Yli-Pirila, P., Kortelainen, M., Grigonyte, J., Tissari, J.,
757   Lamberg, H., Hartikainen, A., Kuuspalo, K., Kortelainen, A.-M., Virtanen, A.,
758   Lehtinen, K. E. J., Komppula, M., Pieber, S., Prevot, A. S. H., Onasch, T. B.,
759   Worsnop, D. R., Czech, H., Zimmermann, R., Jokiniemi, J., and Sippula, O.:
760   Transformation of logwood combustion emissions in a smog chamber: formation
761   of secondary organic aerosol and changes in the primary organic aerosol upon
762   daytime and nighttime aging, Atmos. Chem. Phys., 16, 13251-13269, doi:
763   10.5194/acp-16-13251-2016, 2016.

764 US EPA: Estimation Programs Interface Suite™ for Microsoft® Windows, v 4.11,
765   United States Environmental Protection Agency, Washington, DC, USA, 2012.

Atmospheric
Chemistry
and Physics
Discussions

766   Wang, D., Zhou, B., Fu, Q., Zhao, Q., Zhang, Q., Chen, J., Yang, X., Duan, Y., and Li,
767   J.: Intense secondary aerosol formation due to strong atmospheric photochemical
768   reactions in summer: observations at a rural site in eastern Yangtze River Delta of
769   China, Sci. Total Environ., 571, 1454-1466, doi: 10.1016/j.scitotenv.2016.06.212,
770   2016.
771   Wang, Y., Hu, M., Lin, P., Guo, Q., Wu, Z., Li, M., Zeng, L., Song, Y., Zeng, L., Wu,
772   Y., Guo, S., Huang, X., and He, L.: Molecular characterization of nitrogen-
773   containing organic compounds in humic-like substances emitted from straw
774   residue   burning,   Environ.   Sci.   Technol.,   51,   5951-5961,   doi:
775   10.1021/acs.est7b00248, 2017.
776   Ward, T. J., Rinehart, L. R., and Lange, T.: The 2003/2004 Libby, Montana PM2.5
777   source apportionment research study, Aerosol Sci. Technol., 40, 166-177, doi:
778   10.1080/02786820500494536, 2006.
779   Xu, L., Middlebrook, A. M., Liao, J., de Gouw, J. A., Guo, H., Weber, R. J., Nenes, A.,
780   Lopez-Hilfiker, F. D., Lee, B. H., Thornton, J. A., Brock, C. A., Neuman, J. A.,
781   Nowak, J. B., Pollack, I. B., Welti, A., Graus, M., Warneke, C., and Ng, N. L.:
782   Enhanced formation of isoprene-derived organic aerosol in sulfur-rich power plant
783   plumes during Southeast Nexus, J. Geophys. Res.-Atmos., 121, 11137-11153, doi:
784   10.1002/2016jd025156, 2016.
785   Yang, B., Zhang, H., Wang, Y., Zhang, P., Shu, J., Sun, W., and Ma, P.: Experimental
786   and theoretical studies on gas-phase reactions of NO_3 radicals with three
787   methoxyphenols: Guaiacol, creosol, and syringol, Atmos. Environ., 125, 243-251,
788   doi: 10.1016/j.atmosenv.2015.11.028, 2016.
789   Yang, Y., Shao, M., Kessel, S., Li, Y., Lu, K., Lu, S., Williams, J., Zhang, Y., Zeng, L.,
790   Noelscher, A. C., Wu, Y., Wang, X., and Zheng, J.: How the OH reactivity affects
791   the ozone production efficiency: case studies in Beijing and Heshan, China, Atmos.
792   Chem. Phys., 17, 7127-7142, doi: 10.5194/acp-17-7127-2017, 2017.
793   Yee, L. D., Kautzman, K. E., Loza, C. L., Schilling, K. A., Coggon, M. M., Chhabra, P.
794   S., Chan, M. N., Chan, A. W. H., Hersey, S. P., Crounse, J. D., Wennberg, P. O.,
795   Flagan, R. C., and Seinfeld, J. H.: Secondary organic aerosol formation from
796   biomass burning intermediates: phenol and methoxyphenols, Atmos. Chem. Phys.,
797   13, 8019-8043, doi: 10.5194/acp-13-8019-2013, 2013.
798   Zhang, H., Yang, B., Wang, Y., Shu, J., Zhang, P., Ma, P., and Li, Z.: Gas-phase reactions
799   of methoxyphenols with NO_3 radicals: Kinetics, products, and mechanisms, J.
800   Phys. Chem. A, 120, 1213-1221, doi: 10.1021/acs.jpca.5b10406, 2016.
801   Zhang, X., Lambe, A. T., Upshur, M. A., Brooks, W. A., Be, A. G., Thomson, R. J.,
802   Geiger, F. M., Surratt, J. D., Zhang, Z., Gold, A., Graf, S., Cubison, M. J., Groessl,
803   M., Jayne, J. T., Worsnop, D. R., and Canagaratna, M. R.: Highly oxygenated
804   multifunctional compounds in alpha-pinene secondary organic aerosol, Environ.
805   Sci. Technol., 51, 5932-5940, doi: 10.1021/acs.est.6b06588, 2017.
806   Ziemann, P. J., and Atkinson, R.: Kinetics, products, and mechanisms of secondary
807   organic   aerosol   formation,   Chem.   Soc.   Rev.,   41,   6582-6605,   doi:

808   10.1039/c2cs35122f, 2012.

Atmospheric
Chemistry
and Physics
Discussions

809 **Table 1.** Rate constant for gas-phase reaction of eugenol with OH radicals and

810 associated atmospheric lifetime.

Compound	Structure	References	k_E/k_R	k_E [a]	k_{OH} [a]	k_E (average) [a]	τ_{OH} (h) [b]
eugenol ($C_{10}H_{12}O_2$)	H₃CO / HO	1,3,5-trimethylbeneze	1.33 ±0.05	7.54 ±0.28	6.50 [c]	8.01 ±0.40	2.31
		m-xylene	3.85 ±0.23	8.47 ±0.51			

811 [a] Units of 10^{-11} cm^3 molecule^{-1} s^{-1}.

812 [b] Atmospheric lifetime in hours. $\tau_{OH}=1/k_E[OH]$, assuming a 24 h average [OH] = 1.5 ×

813 10^6 molecules cm^{-3} (Mao et al., 2009).

814 [c] Calculated using US EPA AOP WIN model (US EPA, 2012).

815 **Table 2.** Experimental conditions and results.

Expt.	[eugenol]$_0$ [a] (µg m^{-3})	Δ[eugenol] [b] (µg m^{-3})	M_0 [c] (µg m^{-3})	Y_{max} [d]	OH Exposure [e] (10^{11} molecules cm^{-3} s)	τ [f] (d)
#1	272	265	29	0.11	5.41	4.17
#2	351	339	54	0.16	5.41	4.17
#3	485	474	83	0.18	5.41	4.17
#4	636	625	145	0.23	5.41	4.17
#5	874	858	241	0.28	7.37	5.68
#6	1327	1304	399	0.31	8.91	6.87

816 [a] Initial eugenol concentrations.

817 [b] Reacted eugenol concentrations.

818 [c] SOA concentrations.

819 [d] Maximum SOA yields.

820 [e] Corresponding OH exposure of maximum SOA yields.

821 [f] Corresponding atmospheric aging time of maximum SOA yields, calculated using a

822 typical [OH] in the atmosphere in this work (1.5×10^6 molecules cm^{-3}) (Mao et al.,
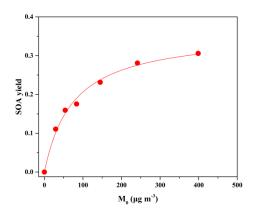
823 2009).

Figure 1. Relative rate plots for gas-phase reaction of OH radicals with eugenol.

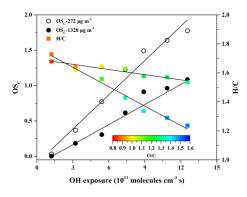**Figure 2.** Maximum SOA yield as a function of SOA mass concentration (M_0) formed

from the OH reactions at different eugenol concentrations. The solid line was fit to the

experimental data using an one-product model. Values for α_i and $K_{om,i}$ used to generate

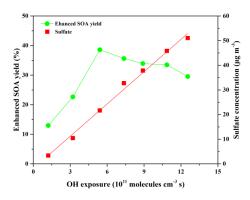the solid line are (0.36 ± 0.02) and (0.013 ± 0.002), respectively.

831

832   **Figure 3.** OS_C, H/C, and O/C vs. the OH exposure for SOA formed at two eugenol

833   concentrations (272 and 1328 $\mu g\ m^{-3}$).
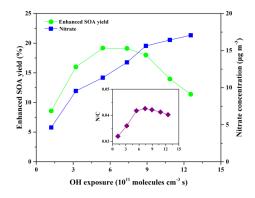

834

835   **Figure 4.** Evolution of the enhanced SOA yield and sulfate formation as a function of

836   OH exposure in the presence of 41 ppbv SO_2 at average eugenol concentration of 273

837    $\mu g\ m^{-3}$.

Atmospheric
Chemistry
and Physics
Discussions

838

Figure 5. Evolution of the enhanced SOA yields, nitrate formation, and N/C ratioas a

function of OH exposure in the presence of 40 ppbv NO_2 at average eugenol

concentration of 273 $\mu g\ m^{-3}$.